eprints@whiterose.ac.uk
https://eprints.whiterose.ac.uk/

Low Multiplication Noise Thin $Al_{0.6}Ga_{0.4}As$ Avalanche Photodiodes

Chee Hing Tan, J. P. R. David, Stephen A. Plimmer, Graham J. Rees, Richard C. Tozer, and Robert Grey

Abstract—Avalanche multiplication and excess noise were measured on a series of $Al_{0.6}Ga_{0.4}As$ p^+in^+ and n^+ip^+ diodes, with avalanche region thickness, w ranging from 0.026 μm to 0.85 μm. The results show that the ionization coefficient for electrons is slightly higher than for holes in thick, bulk material. At fixed multiplication values the excess noise factor was found to decrease with decreasing w, irrespective of injected carrier type. Owing to the wide $Al_{0.6}Ga_{0.4}As$ bandgap extremely thin devices can sustain very high electric fields, giving rise to very low excess noise factors, of around $F \sim 3.3$ at a multiplication factor of $M \sim 15.5$ in the structure with $w = 0.026 \mu$ m. This is the lowest reported excess noise at this value of multiplication for devices grown on GaAs substrates. Recursion equation modeling, using both a hard threshold dead space model and one which incorporates the detailed history of the ionizing carriers, is used to model the nonlocal nature of impact ionization giving rise to the reduction in excess noise with decreasing w. Although the hard threshold dead space model could reproduce qualitatively the experimental results better agreement was obtained from the history-dependent model. p

Index Terms—$Al_xGa_{1-x}As$, avalanche photodiodes, excess noise, impact ionization.

I. INTRODUCTION

AVALANCHE photodiodes (APDs) are widely used in telecommunications systems since the avalanche multiplication process provides gain. Conventionally, the impact ionization coefficients for electrons and holes, α and β, which represent the inverse of the mean distance between successive ionization events, have been used to describe the multiplication process. Using a local analysis, McIntyre [1] derived an expression for the excess avalanche noise factor, F, which arises from the stochastic nature of the ionization process, as a function of mean multiplication, M and $k = (\beta/\alpha)(\alpha/\beta)$ for electron (hole) initiated multiplication

$$F = kM + \left(2 - \frac{1}{M}\right)(1 - k). \tag{1}$$

To minimize the excess noise the material must have a small value of k and therefore the carrier with the higher ionization coefficient must be injected to initiate the multiplication process.

This model assumes that the dead space, d, defined as the minimum distance a carrier must travel before impact ionizing, is small compared with both the avalanche width, w, and with the mean distance between ionization events, so that α and β are in equilibrium with the local electric field.

In most III–V semiconductors k approaches unity at high fields and so to achieve small values of k APDs usually operate at relatively low electric fields, necessitating thick avalanche multiplication regions, where the McIntyre expression is valid. As the avalanche region becomes thinner, d becomes a significant fraction of the avalanche region width and thus the local description of ionization fails. The dead space has been shown to affect the multiplication [2] and, more dramatically, to reduce the excess avalanche noise in thin avalanche regions [3]–[6]. APDs with thin avalanche regions also have the further advantage of a high gain-bandwidth product.

Unfortunately, at the high electric fields encountered in these thin multiplication regions, the tunnelling current can be significant, increasing the background shot noise. One way to overcome this problem is to use a wider bandgap material such as $Al_xGa_{1-x}As$, with consequently reduced tunnelling current. Recently, Heroux *et al.* [7] showed that GaInAs alloyed with a dilute concentration of N and grown on a GaAs substrate strongly absorbs incident light at 1.3 μm wavelength. $Al_xGa_{1-x}As$ could therefore provide an attractive multiplication region for GaAs based APDs using GaInAs(N) absorption regions.

Avalanche multiplication measurements in $Al_xGa_{1-x}As(x < 0.45)$ have been reported by several groups [8]–[12]. Anselm *et al.* [4] have measured the excess noise in $Al_xGa_{1-x}As$ for $x = 0$ and 0.2 and Li *et al.* [6] have measured excess noise in $Al_xGa_{1-x}As$ for $x = 0$ and 0.3. The excess noise in $Al_xGa_{1-x}As$ for $x = 0$ to 0.3 was found to reduce with decreasing w. No measurements of excess noise factor of $Al_xGa_{1-x}As$ with higher aluminum compositions have been reported. The excess noise characteristics for high aluminum compositions ($x > 0.45$) where the bandgap is indirect, is not known at present. In our previous work [12], the multiplication characteristics of $Al_{0.6}Ga_{0.4}As$ have been investigated, and the k value was found to be close to unity even at low electric fields. The dark current of $Al_{0.6}Ga_{0.4}As$ was also found to be very low. Therefore, in this work, we investigate the excess noise in $Al_{0.6}Ga_{0.4}As$ using a range of p^+in^+ diodes with w varying from 0.06 μm to 0.85 μm and n^+ip^+ diodes with w equal to 0.14 μm and 0.51 μm. By fabricating diodes with w ranging from 0.026 μm to 0.85 μm, the multiplication and excess noise characteristics over a wide range of electric fields can be investigated. We have also investigated a p-n diode with
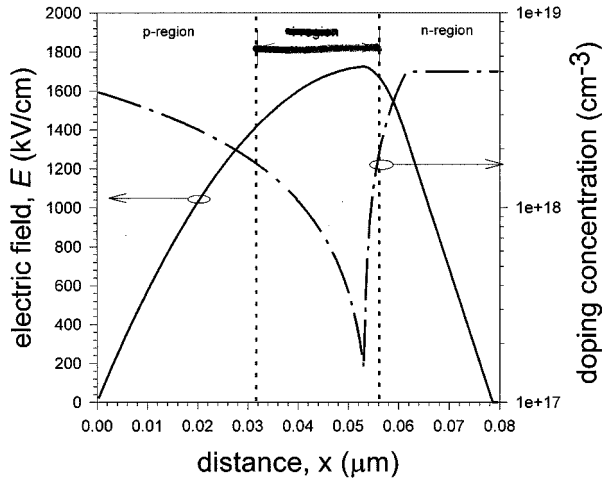
Fig. 1. Doping profile (dash-dot line) in the layer with $w = 0.049\,\mu$m obtained from SIMS and the calculated electric field profile (solid line).

a highly nonuniform electric field. In Section II, we outline the experimental details of this work. The results are presented in Section III, discussed in Section IV, and modeled using a model that includes the field history of the ionizing carrier, proposed by McIntyre [13] in Section V.

II. EXPERIMENTAL DETAILS

A. Growth and Characterization

The $p^+in^+(n^+ip^+)$ layers used in this study were grown by conventional molecular beam epitaxy using Be and Si as the p- and n-type dopants on $n^+(p^+)(001)$ GaAs substrates. A 0.2 μm $n^+(p^+)$ AlAs etch-stop layer was grown on the substrate, followed by a 1.5 μm $n^+(p^+)$ $Al_{0.6}Ga_{0.4}As$ layer, an undoped $Al_{0.6}Ga_{0.4}As$ i-region, and finally 1 μm of $p^+(n^+)$ $Al_{0.6}Ga_{0.4}As$. Circular mesa diodes of diameter 50–400 μm were fabricated, with annular contacts for optical access.

The i-region thickness of each layer was estimated from the doping profile obtained via capacitance–voltage (C–V) measurements. These values were checked by solving Poisson's equation, with w and the doping in the p^+, i, and n^+ regions used as adjustable parameters to fit the measured C–V profiles, as in our previous works [2], [5], [6], [11], [12]. The estimated values of w were 0.026 μm, 0.049 μm, 0.09 μm, 0.49 μm, and 0.85 μm for the p^+in^+ diodes, and 0.14 μm and 0.51 μm for the n^+ip^+ diodes. This fitting exercise also gives the doping levels of the p-n diode as around 4.4×10^{17} cm^{-3} in the p-region and around 1.10×10^{18} cm^{-3} in the n-region. Secondary ion mass spectroscopy (SIMS) measured on several layers also shows good agreement with the values of w obtained via the modeling from C–V measurements. The doping profiles from SIMS also suggest that the layers with $w = 0.026$ μm and 0.049 μm have a rounded electric field profile, as shown in Fig. 1, rather than a uniform electric field profile, because of diffusion of the p and n-type dopants. The details of the layers are summarized in Table I.

Devices from all layers show sharp breakdown and low dark currents ($\approx 10^{-9}$ A) up to the breakdown voltage, as shown in

Parameter	$E < 600$ kV/cm	$E \geq 600$ kV/cm
A_e	4.47×10^6 /cm	3.58×10^6 /cm
E_{ce}	2.80×10^6 kV/cm	2.70×10^6 kV/cm
A_h	3.08×10^6 /cm	3.58×10^6 /cm
E_{ch}	2.84×10^6 kV/cm	2.70×10^6 kV/cm
$E_{th,e}$	4.04 eV	
$E_{th,h}$	4.40 eV	

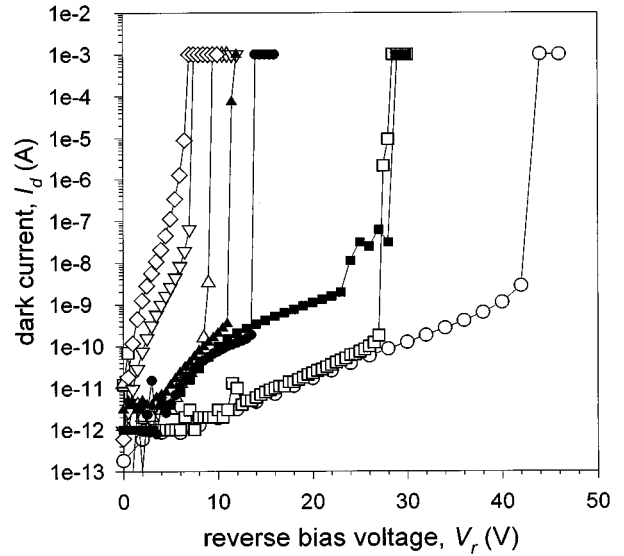Fig. 2. Current–voltage characteristics in dark for $Al_{0.6}Ga_{0.4}As$ p^+in^+ diodes with $w = 0.85$ μm (∘), 0.49 μm (□), 0.09 μm (△), 0.049 μm (▽), 0.026 μm (◇), and n^+ip^+ diodes with $w = 0.51$ μm(■), and 0.14 μm (▲). The current–voltage characteristic of the p-n diode with doping levels of $\approx 4.4 \times 10^{17}$ cm^{-3} in the p-region and $\approx 1 \times 10^{18}$ cm^{-3} in the n-region is also shown (●).

Fig. 2. In the two thinnest layers with $w = 0.026$ μm and 0.049 μm, the dark current increases more rapidly prior to breakdown, possibly due to the onset of tunnelling at the very high electric fields in these layers.

B. Photomultiplication and Excess Noise Measurements

The experimental set-ups used for photomultiplication and excess noise measurements are as described in [5], [6]. A phase sensitive detection (PSD) technique using two lock-in amplifiers was employed to monitor the photocurrent and the multiplication noise independently. The PSD technique isolates the thermal, dark current, and system noise from the measured multiplication noise. Our noise measurement system has a center frequency of 10 MHz and 4 MHz bandwidth.

Pure electron (hole) initiated multiplication $M_e(M_h)$ was achieved by shining light of wavelength 442 nm from a He-Cd laser onto the top cladding region of the $p^+in^+(n^+ip^+)$ diodes. The absorption coefficient of $Al_{0.6}Ga_{0.4}As$ at 442 nm is approximately 1.08×10^5 cm^{-1} [14] and therefore, the light is fully absorbed in the 1 μm $p^+(n^+)$ cladding region. The n^+ cladding regions in the two n^+ip^+ diodes were thinned down

to ~0.6 μm to increase the primary hole photocurrent. The 442 nm light is still strongly absorbed in the 0.6 μm n$^+$ cap, ensuring pure hole injection. Measurements of mixed carrier initiated multiplication M_{mix} were performed on the n$^+$ip$^+$ diodes using 542 nm light from a He-Ne laser which has an absorption coefficient of approximately 2.9×10^4 cm^{-1} [14] in Al$_{0.6}$Ga$_{0.4}$As and therefore, approximately 17.6% of the light entered the high field region. In the p$^+$in$^+$ diodes with $w = 0.85$ μm, and 0.049 μm M_e was obtained without thinning the p$^+$ cladding region but for M_{mix}, this was etched down to a thickness of ~ 0.3 μm so that around 42% of the 542 nm light entered the high field region.

The small increase in primary photocurrent prior to the onset of multiplication due to a slight movement of the depletion edge with increasing bias was corrected for, as described by Woods [15]. The excess noise factor F was determined as in [5], [6] by comparing the shot noise of a commercial silicon pin diode under unity multiplication conditions to that of the test devices using the technique described by Bulman [16]. F can be expressed as

$$F = \frac{i_{\mathrm{eq}}}{M^2 i_{\mathrm{pr}}} \tag{2}$$

where

i_{eq} equivalent photocurrent of a silicon pin diode that produces the same noise power as the device under test;

M equal to M_e, M_h or M_{mix};

i_{pr} unmultiplied photocurrent.

Multiplication and noise measurements were taken from several devices on each layer to ensure reproducibility.

III. RESULTS

The normalized multiplication factors M_e and M_h up to 10 are shown in Fig. 3 although multiplication factors of between 9 to 25 were obtained in all layers. M_{mix} results for the p$^+$in$^+$ diodes with $w = 0.85$ μm and 0.049 μm and for the n$^+$ip$^+$ diodes are also shown in Fig. 3. M_{mix} is slightly lower than M_e in the p$^+$in$^+$ diode with $w = 0.85$ μm but these are almost identical in the thinner p$^+$in$^+$ diode with $w = 0.049$ μm and the n$^+$ip$^+$ diode with $w = 0.14$ μm. In the thicker n$^+$ip$^+$ diode with $w = 0.51$ μm, M_{mix} is slightly higher than M_h. M_e for the p-n diode which breaks down at a reverse bias of 14 V is also shown in the same figure.

The measured pure electron initiated excess noise factor, F_e from the p$^+$in$^+$ diodes is shown in Fig. 4. The excess noise factors for the thickest layer, with $w = 0.85$ μm, fall close to the curve calculated for $k \sim 0.4$ from (1). As w was reduced successively to 0.49 μm, 0.09 μm, 0.049 μm and 0.026 m the excess noise factors were found to decrease and fall close to the calculated curves with $k \sim 0.36$, 0.21, 0.17 and 0.10, respectively. Mixed carrier initiated excess noise, F_{mix} results on the p$^+$in$^+$ diode with w of 0.049 μm and 0.85 μm are compared to F_e in the inset of Fig. 4. F_{mix} was found to be only slightly higher than F_e in the p$^+$in$^+$ diode with $w = 0.049$ μm. However in the thicker p$^+$in$^+$ diode, with $w = 0.85$ μm, the mixed injection produced much higher excess noise, falling on the curve with $k \sim 1.5$.
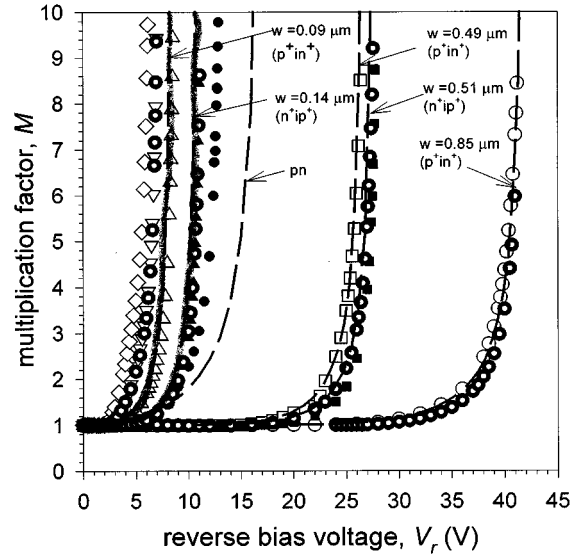

Fig. 3. Multiplication characteristics for pure carrier injection with 442 nm excitation (symbols), mixed carrier injection with 542 nm excitation ($\circ$) and calculated using the DSM with the ionization coefficients and threshold energies, $E_{\mathrm{th,e}} = 3.4$ eV and $E_{\mathrm{th,h}} = 3.6$ eV, from [12] (dashed lines). The measured M_e results are represented by symbols for Al$_{0.6}$Ga$_{0.4}$As p$^+$in$^+$ diodes with $w = 0.85$ μm ($\circ$), 0.049 μm ($\square$), 0.09 μm ($\triangle$), 0.049 μm (∇), 0.026 μm ($\diamond$) and M_h for n$^+$ip$^+$ diodes with $w = 0.51$ μm ($\blacksquare$) and 0.14 μm ($\blacktriangle$), together with M_e for the p-n diode ($\bullet$).

Fig. 4. Excess noise factor, F_e measured (symbols) and calculated (lines) using the DSM with ionization coefficients and threshold energies from [12] for Al$_{0.6}$Ga$_{0.4}$As p$^+$in$^+$ diodes with $w = 0.85$ μm ($\circ$, dashed line), 0.49 μm ($\square$, dotted line), 0.09 μm ($\triangle$, dash-dotted line), 0.049 μm (∇) and 0.026 μm ($\diamond$). Thin dotted lines are curves calculated from (1) for various k values from 0 to 1 in steps of 0.1. The excess noise factors from mixed carrier initiated multiplication (closed symbols) and from pure electron initiated multiplication (open symbols) for the layers with $w = 0.85$ ($\bullet$, $\circ$) μm and 0.049 μm ($\blacktriangledown$, $\triangledown$) are also shown in the inset.

Fig. 5 shows the excess noise results, F_h for pure hole injection of the two n$^+$ip$^+$ diodes with $w = 0.51$ μm and 0.14 μm falling on the curves with $k \sim 0.7$ and 0.3 respectively, and F_e for the p-n diode falling close to curve with $k \sim 0.2$. As before F_{mix} from the n$^+$ip$^+$ diodes is shown in the inset. F_{mix} is lower than F_h in both n$^+$ip$^+$ diodes. For a fixed value of multiplication the difference between F_{mix} and F_h is smaller in the
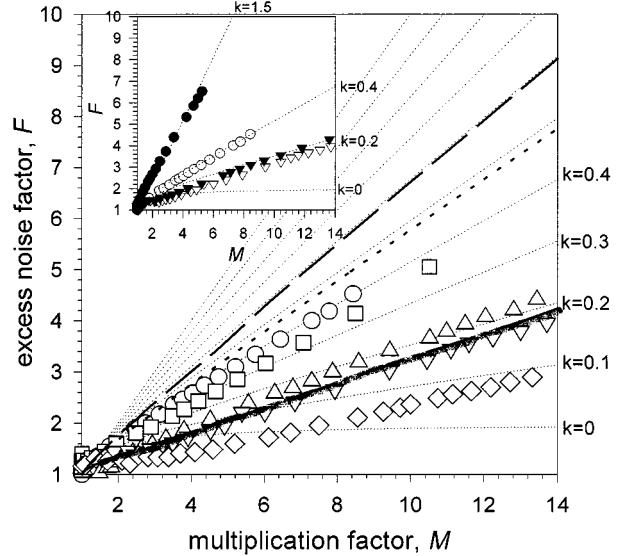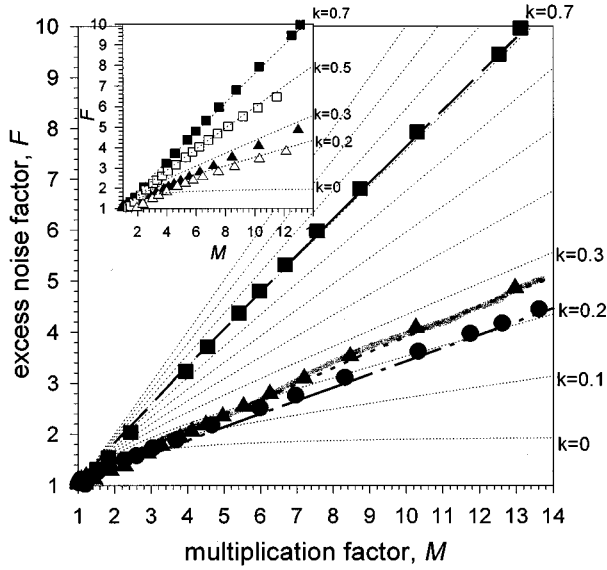
Fig. 5. Excess noise factor, F_h measured (symbols) and calculated (lines) using the DSM with ionization coefficients and threshold energies from [12] for $Al_{0.6}Ga_{0.4}As\ p^+in^+$ diodes with $w = 0.51\ \mu m$ (■, dashed line) and $0.14\ \mu m$ (▲, dotted line), and F_e measured (●) and calculated (dash-dotted line) for the p-n diode. Thin dotted lines are same as for Fig. 4 and the inset shows the excess noise factors from pure hole (closed symbols) and mixed carrier (open symbols) initiated multiplication in the n^+ip^+ diodes with $w = 0.51\ \mu m$ (■, □) and $0.14\ \mu m$ (▲, △).

TABLE II
PARAMETERS FOR THE IONIZATION COEFFICIENTS AND THE THRESHOLD
ENERGIES USED IN THE HISTORY-DEPENDENT MODEL TO FIT THE MEASURED
MULTIPLICATION AND EXCESS NOISE FACTOR IN $Al_{0.6}Ga_{0.4}As$

Parameter	$E < 600$ kV/cm	$E > 600$ kV/cm
A_e	4.47×10^6 /cm	4.67×10^6 /cm
E_{ce}	2.80×10^6 kV/cm	2.95×10^6 kV/cm
A_h	3.08×10^6 /cm	3.58×10^6 /cm
E_{ch}	2.84×10^6 kV/cm	2.70×10^6 kV/cm
$E_{th,e}$	4.04 eV	
$E_{th,h}$	4.40 eV	

ingly important as w decreases. In thin devices, the dead space represents a significant fraction of the avalanche region. Ionization occurs in a narrower spatial region and the multiplication process becomes more deterministic, resulting in reduced spread in the random values of multiplication and hence in reduced noise [17].

The difference between F_{mix} and $F_e(F_h)$ becomes larger as w increases in the $p^+in^+(n^+ip^+)$. This is as expected since the dead space is less significant in the layers with thicker multiplication regions and the α/β ratio dominates the noise characteristics, as discussed by McIntyre [1]. Therefore the mixed carrier initiated multiplication process in the $p^+in^+(n^+ip^+$ diodes will result in higher (lower) F_{mix} than for pure carrier injection in the thicker diodes. The F_e values for the p^+in^+ diode with $w = 0.85\ \mu m$ are lower than those for GaAs and $Al_{0.2}Ga_{0.8}As\,p^+in^+$ diodes with $w = 0.8\ \mu m$ [4], which fall on the curves with $k = 0.48$ and 0.62 in (1) respectively. The reason for this is not clear at present but may be due to a larger d/w ratio in $Al_{0.6}Ga_{0.4}As\,p^+in^+$. To assess this we calculated the d/w ratio for M_e in GaAs, $Al_{0.2}Ga_{0.8}As$ and $Al_{0.6}Ga_{0.4}As\,p^+in^+$ diodes with $w = 0.8$ using the parameters given in [18] and in Table II. For $M_e = 5$ the corresponding calculated d/w ratios were found to be 0.077, 0.065 and 0.096, confirming our hypothesis.

In our earlier work [19] we showed that in pn junctions with rapidly varying electric fields the noise is reduced further as the ionization events are localized in the vicinity of the peak field and thus the impact ionization process becomes even more deterministic. The present p-n diode shows low excess noise, similar to that produced by the p^+in^+ diode with $w = 0.09\ \mu m$, despite a much wider depletion width, for similar reasons.

thinner n^+ip^+ diode. The p-n diode produced very similar results for F_e to those of the p^+in^+ diode with $w = 0.09\ \mu m$, although it has a wider depletion width of $\sim 0.25\ \mu m$ at high multiplication values.

IV. DISCUSSION

The F_e and F_h results clearly show a significant reduction with decreasing w. F_h for the n^+ip^+ diode with $w = 0.14\ \mu m$ is only marginally higher than F_e for the p^+in^+ diode with $w = 0.09\ \mu m$. Note also that F_{mix} is only slightly higher than F_e in the p^+in^+ diode with $w = 0.049\ \mu m$ and only slightly lower than F_h in the n^+ip^+ diode with $w = 0.14\ \mu m$, despite M_{mix} being almost identical to M_e and M_h in the p^+in^+ and n^+ip^+ diodes respectively. These results suggest that the noise performance of $Al_{0.6}Ga_{0.4}As\,p^+in^+$ diodes with $w \leq 0.1\ \mu m$ is largely independent of injected carrier type and depends primarily on w. Similar excess noise results with electron and hole initiated multiplication were observed in GaAs diodes with $w = 0.1\ \mu m$ [5].

To the best of our knowledge the excess noise exhibited by the p^+in^+ diode with $w = 0.026\ \mu m$ is the lowest reported in GaAs based p^+in^+ diodes. Previous attempts at measuring F in $Al_xGa_{1-x}As$ were confined to devices with w no thinner than $0.05\ \mu m$ [5], [6] because the large electric fields in thinner devices gave rise to prohibitively large dark currents. In the wider bandgap $Al_{0.6}Ga_{0.4}As$ extremely thin avalanching regions are achieved with negligible dark currents, as shown in Fig. 2, and an extremely low noise figure was obtained in devices with $w = 0.026\ \mu m$, as shown in Fig. 4.

The reduced excess noise in thin multiplication regions can be explained by the dead space effect which becomes increas-

V. MODELING

The effect of the nonlocal ionization behavior on mean gain was discussed by Okuto and Crowell [20]. Since then several analytical [5], [21]–[24] and numerical techniques [17], [25], [26] have been proposed to model the nonlocal nature of impact ionization.

A simple model for a carrier's nonlocal ionization behavior is to set the ionizing probability to zero for a distance d after the carrier is created, where $d = E_{th}/qE$ is the ballistic distance required to achieve ionization threshold energy, E_{th} in the electric field, E. After travelling this dead space the ioniza-

tion process is described by the ionization coefficients for electrons $(\alpha^*(E))$ and for holes $(\beta^*(E))$. This hard threshold dead space model (DSM) has been used by several authors [5],[6], [22]–[24]. The DSM has been shown to give good fits to the measured gains and excess noise factors in uniform electric field structures [5],[6],[27] and so was used to model our measured multiplication and excess noise results. Using the DSM M_e and M_h were calculated for diodes with w of 0.09 μm to 0.85 μm with the ionization coefficients, $\alpha^*(E)$ and $\beta^*(E)$, and the ionization threshold energies for electrons and holes, $E_{\mathrm{th,e}} = 3.4$ eV and $E_{\mathrm{th,h}} = 3.6$ eV, given by Plimmer *et al.* [12]. The calculated M_e and M_h for ideal p^+in^+ diodes with w of 0.09 μm to 0.85 μm are shown as dashed lines in Fig. 3.

The DSM modified for nonuniform electric fields as described in [23] was used to model the experimental results from the p-n diode. In a nonuniform electric field, $E(x)$ the ballistic dead space is found by solving for d in the equation

$$q \int_x^{x+d} E(x)dx = E_{\mathrm{th}}.$$

The DSM is able to give good agreement with the measured multiplication values for w of 0.09 μm to 0.85 μm but gives values which underestimate the multiplication for the p-n diode. The DSM also predicts higher excess noise in the p^+in^+ diodes with $w = 0.49$ μm and 0.85 μm, as shown in Fig. 4. This suggests that a simple hard threshold DSM is not adequate to account for the nonlocal behavior in our p-n diode. While the hard threshold DSM correctly predicts a reduction in excess noise with decreasing w the detailed agreement is poor. It is possible to improve the fit to the experiment results with different values of ionization coefficients and threshold energies but satisfactory agreement with both the multiplication and excess noise in structures with nonuniform electric fields is unlikely. An alternative to the simple hard threshold dead space model is thus required to account for the strong nonlocal effects found in structures with highly nonuniform electric fields.

Let $\alpha(x', x)$ represent the ionization coefficient at position x of an electron injected cold at an upstream position $x' < x$. $\alpha(x', x)$ will depend on the varying electric field which heats the electron as it travels from x' to x, although the effect of the field at the more recent points on the trajectory will clearly be more important. McIntyre [13] recently proposed a method of accounting for this 'history dependence' of the ionization coefficient by supposing that the value of $\alpha(x', x)$ can be described in terms of an effective electric field, $E_{\mathrm{eff,e}}(x', x)$ at the ionization position, x. $E_{\mathrm{eff,e}}(x', x)$ is calculated as a sum over the fields, $E(\zeta)$ felt by the electron along its trajectory, $x' < \zeta < x$, weighted by a correlation function f_e, which emphasises the carrier's more recent history. Thus

$$E_{\mathrm{eff,e}}(x', x) = \int_{x'}^x E(\zeta)f_e(x - \zeta)d\zeta, \tag{3}$$

where f_e is normalized to unity by

$$\int_0^\infty f_e(\xi)d\xi = 1. \tag{4}$$

The dependence of $\alpha(E_{\mathrm{eff,e}})$ upon the effective field, $E_{\mathrm{eff,e}}$ is taken as that of the equilibrium ionization coefficient on a constant electric field, E, for distances long after the dead space. This is conveniently parametrised by $\alpha(E) = A_e \exp(-E_{\mathrm{ce}}/E)$, where A_e and E_{ce} are constant fitting parameters.

McIntyre proposed a Gaussian correlation function, $f_e(\xi) = (2/\lambda_e\sqrt{\pi}) \exp\left(-(\xi^2/\lambda_e^2)\right)$, with a correlation length, λ_e chosen so that in a constant electric field, E, $\alpha(E_{\mathrm{eff,e}})$ reaches one half of its equilibrium value, $\alpha(E)$ after the ballistic dead space, $d_e = E_{\mathrm{th,e}}/(qE)$, where $E_{\mathrm{th,e}}$ is the electron threshold energy for ionization. As a result λ_e is given by the expression

$$\lambda_e = \frac{\left(\dfrac{E_{\mathrm{th,e}}}{qE}\right)}{\mathrm{erf}^{-1}\left(\dfrac{E_{\mathrm{ce}}}{E_{\mathrm{ce}}+E\ln(2)}\right)}. \tag{5}$$

Over the range of electric fields and parameters we consider the denominator is of order unity and we take, to a reasonable approximation,

$$\lambda_e(\zeta) = \left(\frac{E_{\mathrm{th,e}}}{qE(\zeta)}\right) \tag{6}$$

so that the correlation length is just given by the dead space in the electric field $E(\zeta)$ at position ζ. This dependence of correlation length on position on the trajectory is included in evaluating the effective electric field, $E_{\mathrm{eff,e}}(x)$.

The probability distribution function for ionization is then given by

$$p_e(x', x) = \alpha(x', x)\exp\left(-\int_{x'}^x \alpha(x', \zeta)d\zeta\right). \tag{7}$$

Similar arguments apply to holes. Once the probability of ionizing for both electrons and holes in this history-dependent model are calculated the multiplication and excess noise factor can be calculated by solving the recurrence equations as given in [22], [23].

In this history-dependent model, for devices with $w = 0.09$–0.85 μm, the electric field is assumed to be constant with negligible depletion into the cladding regions while the SIMS doping profile was used to calculated the electric field in the two thinnest layers with $w = 0.026$ μm and 0.049 μm. Ionization threshold energies $E_{\mathrm{th,e}} = 4.04$ eV and $E_{\mathrm{th,h}} = 4.40$ eV give good fit to our measured results and are approximately twice the bandgap. The values of $E_{\mathrm{th,e}}$, $E_{\mathrm{th,h}}$, A_e, E_{ce}, A_h and E_{ch}, where A_h and E_{ch} are the constant fitting parameters of the hole ionization coefficient, are summarized in Table II. Excellent agreement was achieved for the multiplication in all layers as shown in Fig. 6. The calculated excess noise is now also in excellent agreement with the experimental results for all except the two thinnest layers. The calculated F_e in the layer with $w = 0.049$ μm is slightly higher than measured but in the thinnest layer with $w = 0.026$ μm, the calculated F_e is significantly higher than the measured. The reason for this is not obvious at present. A small change to the electric field profile had no significant effect on F_e although
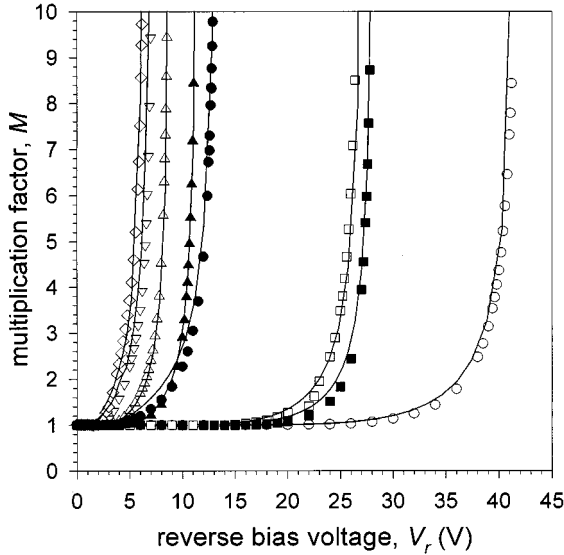
Fig. 6. Comparison between the modeled multiplication factors using the history-dependent model (solid lines), and the experimental results (symbols) for $Al_{0.6}Ga_{0.4}As p^{+}in^{+}$ diodes with $w = 0.85$ μm (o), 0.49 μm ($\square$), 0.09 μm ($\triangle$), 0.049 μm (∇), 0.026 μm ($\diamond$), and $n^{+}ip^{+}$ diodes with $w = 0.51$ μm ($\blacksquare$), and 0.14 μm ($\blacktriangle$), together with the p-n diode ($\bullet$).

it appeared to change M_{e} more substantially in these layers. The discrepancies between the calculated and measured values of F_{e} may be due to inaccuracies in the parameters given in Table II at very high electric fields since the peak electric field in these two layers is > 1000 kV/cm. Note that using different values of α and β as a result of increasing E_{ch} or decreasing E_{ce} at fields > 1000 kV/cm could give a better fit to the measured value of F_{e} in the $p^{+}in^{+}$ diodes with $w = 0.026$ μm and 0.049 μm. However, increasing E_{ch} or decreasing E_{ce} will also result in a higher F_{h} and lower M_{h} at the same electric field. This is not realistic since M_{e} and M_{h} are very similar at such high fields and consequently, we cannot arbitrarily alter E_{ch} and E_{ce}. Therefore, measured data for M_{e}, M_{h}, F_{e}, and F_{h} are essential in order to obtain unambiguous expressions for $\alpha(E)$ and $\beta(E)$.

To test the history-dependent model further, we used this model with the parameters shown in Table II to compare with the measured data from the highly nonuniform electric field in the p-n diode. Figs. 6 and 7 show the good agreement obtained, although this model predicts slightly higher M_{e} just below breakdown. The results show that this model is able to account for the nonlocal behavior of impact ionization in both the uniform and nonuniform electric field structures in all except the two thinnest layers. The history-dependent ionization coefficients used in this model are also plotted in Fig. 8 and compared to the expressions given by Plimmer et al. [12]. These ionization coefficients are only slightly higher than those given by Plimmer et al., obtained using a Monte Carlo technique to reproduce their multiplication results in a wide range of w. Therefore, this model can be used to extract the "microscopic" ionization coefficients $\alpha^{*}(E)$ and $\beta^{*}(E)$, which can be used in recursion equation modeling. The correlation function in this history-dependent model also tracks the history of the carriers in a more realistic manner
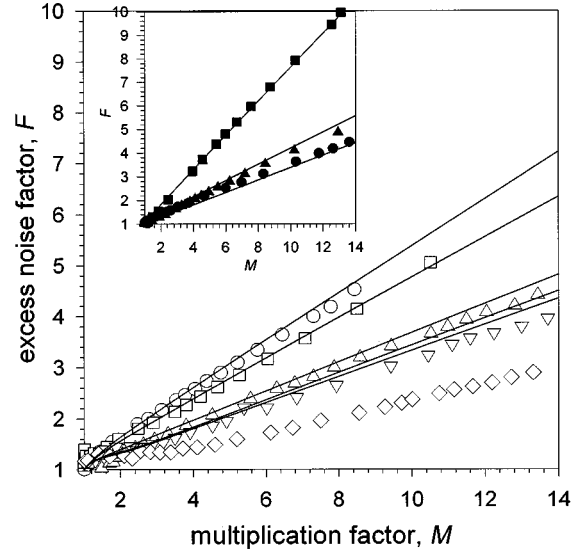

Fig. 7. Modeled excess noise factor (solid lines) using the history-dependent model for $Al_{0.6}Ga_{0.4}As p^{+}in^{+}$ diodes with $w = 0.85$ μm(o), 0.49 μm ($\square$), 0.09 μm ($\triangle$), 0.049 μm (∇), 0.026 μm ($\diamond$) and $n^{+}ip^{+}$ diodes with $w = 0.51$ μm ($\blacksquare$) and 0.14 μm ($\blacktriangle$), and for the p-n diode ($\bullet$).
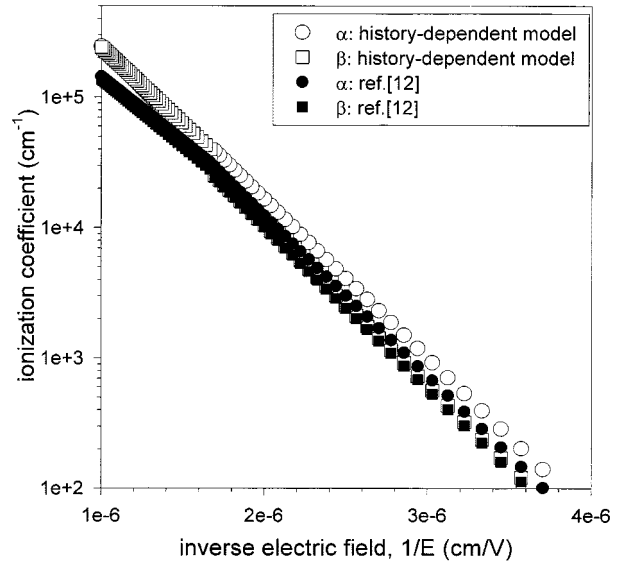
Fig. 8. Comparison of the fitted ionization coefficients for electrons (o) and holes ($\square$) in the history-dependent model with the expression given by [12] (closed symbols).

than a simple hard threshold DSM giving better fits to the experimental results.

VI. CONCLUSION

Pure electron and hole-initiated avalanche multiplication and excess noise measurements were performed on a series of $Al_{0.6}Ga_{0.4}As$ diodes with w ranging from 0.85 μm down to 0.026 μm and also on a p-n diode. The excess noise was found to decrease as w decreases in these layers in a manner similar to that in GaAs and $Al_{x}Ga_{1-x}As$ for $x = 0$ to 0.3 reported previously. This is attributed to the increased importance of dead space as w decreases, which results in a narrower ionization probability distribution function and hence a more

deterministic multiplication process. The p-n diode, which has a highly nonuniform electric field exhibited and very low noise, is comparable to the excess noise of a p^+in^+ diode with 0.09 μm in spite of having a wider depletion width of ~ 0.25 μm. The wide band gap of $Al_{0.6}Ga_{0.4}As$ enables very thin structures with negligible tunneling currents to be realized, and consequently, extremely low noise can be achieved.

Avalanche multiplication and excess noise was modeled using a hard threshold dead space model and a model that incorporates the electric field history of an ionizing carrier. The DSM was able to reproduce the measured multiplication and excess noise qualitatively but was unsatisfactory in the very thin structures and in the p-n diode. A much better fit to our measured multiplication and excess noise was obtained using the history-dependent model, suggesting that the nonlocal behavior has been appropriately accounted for. Although the history-dependent model can give good fits to measured results without using the ionization coefficients as input parameters, data from both electron and hole-initiated avalanche processes is needed to provide unambiguous expressions for $\alpha(E)$ and $\beta(E)$.

ACKNOWLEDGMENT

REFERENCES

[1] R. J. McIntyre, "Multiplication noise in uniform avalanche diodes," *IEEE Trans. Electron Devices*, vol. ED-13, pp. 164–168, Jan. 1966.

[2] S. A. Plimmer, J. P. R. David, D. C. Herbert, T.-W. Lee, G. J. Rees, P. A. Houston, R. Grey, P. N. Robson, A. W. Higgs, and D. R. Wright, "Investigation of Impact ionization in thin GaAs diodes," *IEEE Trans. Electron Devices*, vol. 43, pp. 1066–1072, July 1996.

[3] C. Hu, K. A. Anselm, B. G. Streetman, and J. C. Campbell, "Noise characteristics of thin multiplication region GaAs avalanche photodiode," *Appl. Phys. Lett.*, vol. 69, pp. 3734–3737, 1996.

[4] K. A. Anselm, H. Nie, C. Hu, C. Lenox, P. Yuan, G. Kinsey, J. C. Campbell, and B. G. Streetman, "Performance of thin separate absorption, charge, and multiplication avalanche photodiodes," *IEEE J. Quantum Electron.*, vol. 34, pp. 482–450, Mar. 1998.

[5] K. F. Li, D. S. Ong, J. P. R. David, G. J. Rees, R. C. Tozer, P. N. Robson, and R. Grey, "Avalanche multiplication noise characteristics in thin GaAs p^+-I-n^+ Diodes," *IEEE Trans. Electron Devices*, vol. 45, pp. 2102–2107, Oct. 1998.

[6] ——, "Low noise GaAs and $Al_{0.3}Ga_{0.7}As$ avalanche photodetectors," *Proc. Inst. Elect. Eng. Optoelectron.*, vol. 146, no. N0.1, pp. 21–24, 1999.

[7] J. B. Heroux, X. Yang, and W. I. Wang, "GaInNA's resonant-cavity-enhanced photodetector operating at 1.3 μm," *Appl. Phys. Lett.*, vol. 75, no. 18, pp. 2716–2718, 1999.

[8] S. N. Shabde and C. Yeh, "Ionization rates in $(Al_xGa_{1-x})As$," *J. Appl. Phys.*, vol. 41, no. 11, pp. 4743–4744, 1970.

[9] J. P. R. David, J. S. Marsland, H. Y. Hall, N. J. Mason, M. A. Pate, J. S. Roberts, P. N. Robson, J. E. Stitch, and R. C. Woods, "Measured ionization coefficients in $Ga_xAl_{1-x}As$," in *Proc. 1984 Synop. GaAs and Related Compounds*, 1985, p. 247.

[10] V. M. Robbins, S. C. Smith, and G. E. Stillman, "Impact ionization in $Al_xGa_{1-x}As$ for $x = 0.1 - 0.4$," *Appl. Phys. Lett.*, vol. 52, no. 4, pp. 296–298, 1988.

[11] S. A. Plimmer, J. P. R. David, G. J. Rees, R. Grey, D. C. Herbert, D. R. Wright, and A. W. Higgs, "Impact ionization in thin $Al_xGa_{1-x}As$ ($x = 0.15$ and 0.30) P^+-I-N^+s," *J. Appl. Phys.*, vol. 82, no. 3, pp. 1231–1235, 1997.

[12] S. A. Plimmer, J. P. R. David, R. Grey, and G. J. Rees, "Avalanche multiplication in $Al_xGa_{1-x}As$ ($x = 0$ to 0.60)," *IEEE Trans. Electron Devices*, vol. 47, pp. 1089–1097, May 2000.

[13] R. J. McIntyre, "A new look at impact ionization—Part I: A theory of gain, noise, breakdown probability, and frequency response," *IEEE Trans. Electron Devices*, vol. 46, pp. 1623–1631, Aug. 1999.

[14] D. E. Aspnes, S. M. Kelso, R. A. Logan, and R. Bhat, "Optical properties of $Al_xGa_{1-x}As$," *J. Appl. Phys.*, vol. 60, no. 2, pp. 754–766, 1986.

[15] M. H. Woods, W. C. Johnson, and M. A. Lambert, "Use of a Schottky barrier to measure impact ionization coefficients in semiconductors," *Solid State Electron.*, vol. 16, pp. 381–385, 1973.

[16] G. E. Bulman, V. M. Robbins, and G. E. Stillman, "The determination of impact ionization coefficients in (100) gallium arsenide using avalanche noise and photocurrent multiplication measurements," *IEEE Trans. Electron Devices*, vol. ED-32, pp. 2454–2466, Nov. 1985.

[17] D. S. Ong, K. F. Li, G. J. Rees, G. M. Dunn, J. P. R. David, and P. N. Robson, "A Monte Carlo investigation of multiplication and noise in thin p^+-I-n^+ GaAs avalanche photodiodes," *IEEE Trans. Electron Devices*, vol. 45, pp. 1804–1810, Aug. 1998.

[18] P. Yuan, C. C. Hansing, K. A. Anselm, C. V. Lenox, H. Nie, A. L. Holmes Jr, B. G. Streetman, and J. C. Campbell, "Impact ionization characteristics of III–V semiconductors for a wide range of multiplication region thicknesses," *IEEE J. Quantum Electron.*, vol. 36, pp. 198–204, Feb. 2000.

[19] S. A. Plimmer, C. H. Tan, J. P. R. David, K. F. Li, R. Grey, and G. J. Rees, "The effect of an electric field gradient on avalanche noise," *Appl. Phys. Lett.*, vol. 75, no. 19, pp. 2963–2965, 1999.

[20] Y. Okuto and C. R. Crowell, "Ionization coefficients in semiconductors: A nonlocal property," *Phys. Rev. B*, vol. 10, pp. 4284–4296, 1974.

[21] J. S. Marsland, R. C. Wood, and C. A. Brownhill, "Lucky drift estimation of excess noise factor for conventional avalanche photodiodes including the dead space," *IEEE Trans. Electron Devices*, vol. 39, pp. 1129–1134, May 1992.

[22] M. M. Hayat, B. E. A. Saleh, and M. C. Teich, "Effect of dead space on gain and noise of double-carrier multiplication avalanche photodiodes," *IEEE Trans. Electron Devices*, vol. 39, pp. 546–552, Mar. 1992.

[23] M. M. Hayat, W. L. Sargeant, and B. E. A. Saleh, "Effect of dead space on gain and noise in Si and GaAs avalanche photodiodes," *IEEE J. Quantum Electron.*, vol. 28, pp. 1360–1365, May 1992.

[24] A. Spinelli and A. L. Lacaita, "Mean gain of avalanche photodiodes in a dead space model," *IEEE Trans. Electron Devices*, vol. 43, pp. 23–30, Jan. 1996.

[25] H. Shichijo and K. Hess, "Band-structure-dependent transport and impact ionization in GaAs," *Phys. Rev. B*, vol. 23, pp. 4197–4207, 1981.

[26] N. Sano, T. Aoki, M. Tomizawa, and A. Yoshii, "Electron transport and impact ionization in Si," *Phys. Rev. B*, vol. 41, no. 17, pp. 12 122–12 128, 1990.

[27] M. A. Saleh, M. M. Hayat, B. E. A. Saleh, and M. C. Teich, "Dead-space-based theory correctly predicts excess noise factor for thin GaAS and AlGaAs avalanche photodiodes," *IEEE Trans. Electron Devices*, vol. 47, pp. 625–633, Mar. 2000.

Chee Hing Tan was born in Raub, Pahang, Malaysia, in 1975. He received the B.Eng. (hons.) degree in electronic engineering from the Department of Electronic and Electrical Engineering, the University of Sheffield, Sheffield, U.K., in 1998, where he is currently pursuing the Ph.D. degree

Currently, he is with the University of Sheffield in the third year of the Ph.D. program, working on experimental and theoretical investigation of excess noise in Si and $Al_xGa_{1-x}As$.

Mr. Tan is a student member of IOP.

J. P. R. David received the B.Eng. and Ph.D. degrees from the Department of Electronic and Electrical Engineering, University of Sheffield, Sheffield, U.K., in 1979 and 1983, respectively.

In 1983, he joined the Department of Electronic and Electrical Engineering, the University of Sheffield, where he was a Research Assistant investigating impact ionization. In 1985, he became responsible for characterization within SERC (now EPSRC) Central Facility for III–V Semiconductors at the same university. His current research interests are piezoelectric III–V semiconductors and impact ionization in bulk and multilayer structures.

Stephen A. Plimmer received the B.S. degree in physics and the Ph.D. degree in experimental and theoretical research, both from the University of Sheffield, Sheffield, U.K., in 1993 and 1997, respectively. His Ph. D rsearch was on impact ionization in $Al_xGa_{1-x}As$ ($x = 0$–0.60).

He did his postdoctoral research on looking at the physics of high field transport in avalanching structures, especially APDs and SPADs. To date, this work has contributed to over 25 journal and conference papers. He now works at a telecommunications consultancy, largely working on varied fixed and mobile wireless technologies.

Graham J. Rees was received the B.A. in physics from Oxford University, Oxford, U.K., in 1966, and the Ph.D. in theoretical physics from Bristol University, Bristol, U.K., in 1969.

He was awarded a one-year Royal Society Exchange Fellowship at the Universita delle Scienze, Rome, Italy, and then lectured for a year in Mathematics at Imperial College, London, U.K.. In 1971, he moved to the Plessey Company's Device Research Laboratory, Caswell, U.K., to Head the Theoretical Technology Group. After visiting fellowships to Lund, Sweden, and the Clarendon Laboratory, Oxford, U.K., he joined the Department of Electronic and Electrical Engineering, University of Sheffield, Sheffield, U.K., in 1991, and was appointed to a personal chair in 1999. His research interests include piezoelectric strained layer semiconductor devices, avalanche photodiodes, and modeling of semiconductor device physics.

Richard C. Tozer received the B.Eng., M.Eng., and Ph.D. degrees from University of Sheffield, Sheffield, U.K., in 1970, 1972, and 1975, respectively.

Following a period of postdoctoral research at the University of Sheffield in the area of CCD device applications, he became a Lecturer at the University of Essex, Essex, U.K., where he researched active sound cancellation. He returned to Sheffield as a Lecturer in 1980, where he teaches analogue circuit design. His research involves the application of analog circuits to a wide range of experimental and instrumental problems and is currently centred around APD noise measurement systems and novel excitation modes for fluorescent lamps.

Dr. Tozer is a Chartered Engineer and a member of the IEE.

Robert Grey received the B.Sc. degree in physics and the Ph.D. degree, both from the University of Newcastle, Newcastle, U.K., in 1973 and 1977, respectively.

From 1977 to 1988, he was with VG Instruments, initially as a Test and Development Scientist, then as a Molecular Beam Epitaxy (MBE) Engineering Manager, and finally taking a role of Customer Services Manager. He moved to the EPSRC Central Facility for III-V semiconductors as an MBE semiconductor crystal grower in 1988, where he provides semiconductor structures for U.K. and international physics and electronics device groups